Applications in Energy and Combustion Science 16 (2023) 100216

Contents lists available at ScienceDirect

Applications in Energy and Combustion Science

journal homepage: www.sciencedirect.com/journal/applications-in-energy-and-combustion-science

# Development of a diesel surrogate for improved autoignition prediction: Methodology and detailed chemical kinetic modeling

Goutham Kukkadapu [a], Russell Whitesides [a], Mengyuan Wang [b,c,*], Scott W. Wagnon [a], Marco Mehl [a,e], Charles K. Westbrook [a], Robert McCormick [d], Chih-Jen Sung [b], William J. Pitz [a]

[a] Lawrence Livermore National Laboratory, Livermore, CA 94551, USA
[b] Department of Mechanical Engineering, University of Connecticut, Storrs, CT 06269, USA
[c] School of Energy and Power Engineering, Beihang University, Beijing 100191, China
[d] National Renewable Energy Laboratory, Golden, CO 80401, USA
[e] Politecnico di Milano, Milano 20133, Italy

ARTICLE INFO

*Keywords:*
Diesel
Diesel surrogate
Detailed kinetic model
Rapid compression machine
Surrogate optimization

ABSTRACT

While the surrogate fuel approach has been successfully applied to the simulation of the combustion behaviors of complex gasoline and jet fuels, its application to diesel fuels has been challenging. One of the main challenges derives from the large molecular size of the representative surrogate components necessary to simulate diesel blends, as the development of detailed chemical kinetic models and their validation becomes more complex. In this study, a new surrogate mixture that emulates the chemical and physical properties of a well-characterized diesel fuel is proposed. An optimization procedure was used to select surrogate components that can match both the physical and chemical properties of the target diesel fuel comprehensively. The surrogate fuel mixture composition was designed to have fuel properties (e.g., boiling point, cloud point, etc.) that enable its use in future diesel engine experiments. A detailed kinetic model for the surrogate fuel mixture was developed by combining well-validated sub-mechanisms of each surrogate component from Lawrence Livermore National Laboratory. The ability of the surrogate mixture and kinetic model to emulate ignition delay times was assessed by comparing the simulated results with measurements for the target diesel fuel. Comparison of the experimental and simulated ignition delay times shows that the current surrogate mixture and kinetic model well capture the autoignition response of the target diesel fuel at varying conditions of pressure, temperature, oxygen concentration, and fuel concentration. The current study is one of the first to demonstrate the efficacy of detailed chemical kinetics for diesel range fuels by assembling validated sub-mechanisms for palette compounds and successfully simulating the autoignition characteristics of a target diesel fuel. The experimental ignition delay times of diesel measured with a rapid compression machine, the surrogate mixture, and the kinetic model developed shall aid in progress of understanding diesel ignition under engine relevant conditions.

## Introduction

The use of computational models able to predict combustion processes can speed up and cut the costs associated to the development of advanced internal combustion engines by reducing the need for engine hardware testing. Despite the continuous improvement of computational platforms, engine simulations remain challenging, as they need to properly predict physical effects such as fuel spray break-up and evaporation, as well as chemical effects such as the complex interactions of turbulent flows and chemical kinetics of multi-component transportation fuels [1,2]. Engine performance is known to be affected by the chemical composition and ignition behavior of the fuel. As transportation fuels like gasoline, diesel, and jet fuels may contain thousands of hydrocarbon components of varying molecular classes, chain lengths, and structural properties [1], the development of a detailed chemical kinetic model to simulate each component with full fidelity is a daunting task. One popular method of simplification employs "surrogate mixtures" that match key properties of the real, "target" fuel. This approach begins with the formulation of a surrogate mixture with a relatively small number of components (generally no more than

* Corresponding author.
*E-mail address:* mengyuanwang@buaa.edu.cn (M. Wang).

https://doi.org/10.1016/j.jaecs.2023.100216
Received 23 February 2022; Received in revised form 29 September 2023; Accepted 18 October 2023
Available online 19 October 2023

10), whose composition is refined to best emulate the desired properties of the target fuel [3]. A chemical kinetic model containing the relevant oxidation chemistry of the surrogate components can then be used to simulate the combustion process of the real fuel. This approach proved to be successful in emulateing gasoline and jet fuels [e.g., 4–6] combustion behavior, leading to significant progress in understanding and modeling the combustion characteristics of these real fuels.

However, progress in modeling of diesel fuels through surrogates has been slower, because the molecular classes and carbon numbers ($C_9$—$C_{22}$) observed typically in diesel fuels are more complex compared to species in gasoline and jet fuels. Fundamental combustion experiments of diesel surrogate components and complex diesel fuels at engine-relevant conditions are often impeded by the low volatilities and high melting points of the fuels. Theoretical studies of diesel surrogate components are also challenging, as they typically scale in computational cost according to the number of heavy atoms constituting the fuel molecules. The number of species and reactions required to assemble a detailed chemical kinetics model of more than a small number of diesel surrogate components is also typically prohibitive for most kinetic modeling efforts. Moreover, the complex alkyl-substituted aromatics and alkyl-substituted cycloalkanes relevant to diesel surrogate fuels are not typically considered because validated kinetic mechanisms may not be available. This combined lack of fundamental data, theory, and kinetic models for representative surrogate components may have led to this lack of progress in diesel surrogate modeling, according to a literature review of diesel surrogate fuels by Pitz and Mueller [1].

Diesel surrogate models proposed in previous literature studies have used simplified compositions of fuel components that have available kinetic models, and only limited physical and chemical properties of their target diesel fuels can be matched. Most of those literature studies have been summarized in our previous work [7]. It can be concluded that those previous studies focused more on matching the specific aspects of the chemical kinetics characterizing the diesel combustion behavior (e.g. the auto-ignition tendency) rather than physical properties of their target diesel fuels, with limited number of fuel components in a surrogate model at first. Thanks to the rapid advancement in chemical kinetics and computing power, surrogate models with a greater number of fuel components were then established, and hence both physical and chemical properties of the target diesel fuel could be better matched [7].

Concerning the surrogate formulation methodology, Anand et al. [8] developed surrogates for nine fuels for advanced combustion engines aiming at studying low-emission, high-efficiency advanced diesel engine concepts, and the fidelity of the surrogate fuel models was judged based on matching several physical and chemical properties of their target fuels. In the work of Chang et al. [9], a decoupling methodology was employed to construct a skeletal oxidation mechanism for a diesel surrogate fuel model. The design of this fuel model focused on matching the chemical characteristics of diesel fuel with less emphasis on physical characteristics, and its mechanism was validated based on various fundamental experiments for the single components and for the fuel mixture, as well as for a practical diesel fuel under wide operating conditions. Mueller et al. [3,10] provided a methodology for formulating, blending, and characterizing a set of four diesel surrogate fuels with improved fidelity in matching the molecular structures, ignition quality, and distillation characteristics of target diesel fuels. In the study of Jameel et al. [11], three diesel surrogates have been formulated by matching five important functional groups in diesel fuels, while the surrogate components were minimized to two species. Those surrogates were experimentally evaluated by various physical and combustion properties, and it has been demonstrated that fewer species in surrogates can be as effective as more complex surrogates. Bai et al. [12] formulated a skeletal mechanism for a tri-component diesel surrogate fuel based on a decoupling methodology, and their skeletal mechanism was further verified against various fundamental combustion experiments. In the investigation of Qian et al. [13], a new methodology for diesel surrogate formulation was proposed by considering not only the physical and chemical properties of the target diesel fuel, but also fuel properties combined with real engine combustion characteristics. Three diesel surrogates were developed and were found to accurately reproduce the engine combustion process. Yu et al. [14,15] and Wang et al. [16] investigated the autoignition characteristics of the three diesel surrogates developed in [13] by using a rapid compression machine (RCM) and a shock tube, and a more recent study of Zhu et al. [17] developed a skeletal mechanism based on the components and experimental ignition behavior of those three diesel surrogates. This skeletal mechanism has been validated against various experimental results, including ignition delay times, species concentration profiles, laminar flame speeds, and actual engine data.

It is noted that those literature studies [3,8–17] were either limited to the diesel surrogate formulation, or only provided skeletal mechanisms of diesel surrogates for the simulation of real diesel combustion. When taking the computational cost into consideration, skeletal mechanisms, with the chemical kinetics simplified accordingly, are directly utilized in computational fluid dynamics approaches for modeling real engine instead of detailed reaction mechanisms. However, detailed chemical kinetic mechanisms are still needed as the starting point for the development of skeletal and reduced mechanisms. In addition, as the chemical reactor network approach, for instance, is one of the major ways that detailed chemical kinetic mechanisms can be taken directly into the modeling of real engines [18], and as the utility of tabulated flamelet models [2] has proven to be feasible for using detailed mechanisms in real-engine simulations, the development of detailed chemical kinetic mechanisms for diesel surrogates continues to benefit end-users.

In view of the above, the current diesel surrogate study has undertaken the following major tasks: (1) formulation of a diesel surrogate mixture of a well-characterized, research-grade diesel fuel by following an optimization procedure, (2) development of a detailed chemical kinetic mechanism based on this diesel surrogate, with the sub-mechanism of each fuel composition being carefully validated in our previous work, (3) validation of the current surrogate model by comparing the experimental ignition characteristics of the target diesel fuel with the simulated results, and (4) chemical kinetic analyses of the current surrogate model to identify dominant reactions controlling the reactivity in diesel combustion. Recognizing that physical and chemical properties represent the composition, volatility, and ignition characteristics of the diesel surrogate, they have been measured and/or estimated to closely emulate those of the target diesel fuel. Ignition delay time measurements of this diesel fuel have also been conducted using an RCM over a wide range of conditions, and the autoignition behavior of neat surrogate components, binary/tertiary blends, and real diesel fuel can all be reasonably predicted by the current surrogate model. The RCM-measured ignition delay times of the target diesel fuel can be used as validation datasets for alternate diesel surrogate formulations and chemical kinetic models, while the surrogate reaction model developed herein can be used to simulate the ignition characteristics of other literature surrogates and potentially a variety of diesel fuels. In addition, this is one of the first studies where each sub-mechanism of the surrogate palette has been experimentally validated, yielding a comprehensive and detailed diesel surrogate mechanism that captures the autoignition behavior of real diesel.

## Experimental specifications

Diesel autoignition experiments are conducted in an RCM by compressing the desired gas mixture to elevated pressures and temperatures using a fast-moving pneumatically-driven creviced piston which is brought to rest towards the end of compression (EOC). Post compression, the piston is held stationary and thus autoignition takes place in a constant volume reactor. The entire test facility, including mixture preparation tank, reaction chamber, and connecting manifold, is equipped with heating tapes which, in this study, are used to pre-heat

the system to 420 K. The reaction chamber is equipped with a thermal-shock resistant, dynamic pressure transducer (Kistler 6125C) for dynamic pressure measurements during the experiment. A static pressure transducer (Omega, MMA100V10T2D0T4A6, ±0.05 % accuracy) is located at the manifold of the mixing tank for the preparation of fuel/oxidizer mixture and for the measurement of the pressure of mixture entering the reaction chamber before each run of experiment. The compressed temperature ($T_C$), namely the gas temperature at the EOC, is determined by the "adiabatic core hypothesis" [19]. Under this assumption, the EOC temperature can be calculated by $\ln\left(\frac{P_C}{P_0}\right) = \int_{T_0}^{T_C} \frac{\gamma}{T(\gamma-1)} dT$, based on the measured pressure trace during the compression stroke, where $P_C$ is the pressure at the EOC, $P_0$ is the initial pressure, $T_0$ is the initial temperature, and γ is the temperature-dependent specific heat ratio of the test mixture. The specific heat of the diesel fuel investigated in this study has been estimated using the composition of "V1 diesel surrogate" from Mueller et al. [3]. Further details about the experimental facility and the adiabatic core hypothesis can be found in [7,20–23].

The diesel fuel used in the RCM experiments is a No. 2-D S15 grade diesel emissions-certification fuel from Chevron-Phillips Chemical Co., denoted in this work as CFA (fuel name used as ULSD#2 in [21]). This research-grade diesel was provided by the Coordinating Research Council (CRC). All the physical and chemical specifications of CFA listed in this work are taken from Mueller et al. [3,10]. The mixture preparation, the vaporization check, and other details of the RCM experiments on the autoignition of CFA can be found in our previous work [7].

Table 1 shows the current test conditions for CFA diesel, including equivalence ratios (ϕ), molar percentages of mixture constituents ($X_i$), and compressed pressures ($P_C$). This test matrix was designed to provide insights into the effects of pressure, oxygen concentration, and fuel loading on diesel ignition in the low-to-intermediate temperature range of 660−1000 K and test the fidelity of the developed surrogate model in capturing the autoignition characteristics of the target diesel fuel. It is further noted that the uncertainty of mixture preparation includes the uncertainties of liquid fuel mass, partial pressures of gaseous components, mixing tank volume, and ambient temperature, with their standard deviations being 0.03 g, 1.3 Torr, 0.01 L, and 1.27 °C, respectively, as discussed in Weber et al. [24]. Following the detailed uncertainty analysis method of [24], the uncertainties in mole fraction of CFA fuel is estimated to be around 5 %, the uncertainties for gaseous $O_2$ and $N_2$ are typically less than 1 %, and the uncertainty for equivalence ratio is less than 5 %.

The ignition delay times reported here are deduced from in-cylinder pressure measurements using the Kistler 6125C dynamic pressure transducer in conjunction with a charge amplifier. Fig. 1(a) shows a representative pressure trace of CFA/oxidizer at $P_C = 10$ bar, $T_C = 681$ K, and ϕ = 0.69 with dilution, demonstrating the definitions of ignition delay times used in this study. Both first-stage ($\tau_1$) and total (τ) ignition delay times are recorded as identified by local maxima of time derivative of pressure trace and are reported relative to the time at the EOC. The nonreactive pressure trace of the same experimental condition has also been shown in Fig. 1(a) as a reference. For each reactive set of $P_C$ and $T_C$, the corresponding nonreactive pressure trace is measured by replacing oxygen with nitrogen to characterize the heat transfer effect on the ignition process and to verify that no heat release has occurred during the compression stroke. For each experimental condition, a minimum of four consecutive RCM runs have been conducted and the ignition delay time closest to the average of the runs has been reported and plotted, which can be seen in Fig. 1(b) with representative pressure traces of CFA/oxidizer at $P_C = 20$ bar, $T_C = 699$ K, and ϕ = 1.02 with dilution. After taking the major uncertainties related to ignition delay time measurements into consideration, including the uncertainties in mixture composition, measurements of initial pressure and temperature, and the facility-dependent non-ideal processes during and after compression, the typical scatter in the reported ignition delay time is found to be less than 15 % of the reported ignition delay time value.

**Table 1**
Experimental test matrix for CFA diesel.

| ϕ | Oxidizer | $X_{fuel}$ ( %) | $X_{O2}$ ( %) | $X_{N2}$ ( %) | $P_C$ (bar) |
|---|---|---|---|---|---|
| 0.5 | Air | 0.51 | 20.9 | 78.59 | 10 |
| 0.69 | Diluted | 0.51 | 15.12 | 84.37 | 10 |
| 0.7 | Diluted | 0.36 | 10.47 | 89.17 | 15 |
| 1.02 | Diluted | 0.51 | 10.24 | 89.25 | 10, 15, 20 |
| 2.0 | Diluted | 0.51 | 5.12 | 94.37 | 20 |

## Surrogate formulation methodology

### *Optimization procedure*

In this work, the surrogate formulation is generated via minimization of an objective function defined such that lower values indicate higher fidelity of the resulting surrogate. This approach is similar to that used in previous fuel surrogate studies reported in literature, where the procedure was successfully applied to gasoline [4,5], jet fuel [25–27], and diesel surrogates [3,8,10,28]. The general form of the objective function here adopted is:

$$F(\vec{x}) = \sqrt{\sum_{i=1}^{N} (w_i f_i(\vec{x}))^2}, \quad (1)$$

where $N$ is the number of target functions, $f_i$ representing the ith desired surrogate quality, $w_i$ is the weighting factor selected to increase or decrease the relative importance of the ith target function, and $\vec{x}$ is the vector representing the volume fractions of surrogate components. Most target functions are defined to capture the distances of a surrogate mixture's properties from those of the target fuel:

$$f_i(\vec{x}) = \left|\frac{(\phi_i^t - \phi_i^s)}{\phi_i^t}\right|, \quad (2)$$

where $\phi_i^s$ are the estimated surrogate properties and $\phi_i^t$ are the corresponding target fuel properties. The property targets selected in this study for matching the target CFA fuel include cetane number, estimated using the volume-fraction-weighted linear blending rule [10], H:C ratio, liquid density, carbon types (each with their own target function defined by Eq. (2)), yield sooting index, and advanced distillation curve [29] with the target function of each measured data point defined in Eq. (3). The target property values are provided in the values adopted in the optimization process are also listed in Table 2.

Table  and Table 3.

The weighting factors used in the current study for optimization of surrogate mixture properties have been adjusted iteratively until a good fit is achieved across all target properties. This iterative process hinges on balancing the match of distillation temperatures against the match of carbon type distribution, a challenging task when operating on a limited palette of components. Depending of the specific application, the relative importance of physical properties vs. chemical properties may vary, therefore, as of today, there are no established procedures to identify universal values for these weights. In the attempt of providing a satisfactorily accurate surrogate for a wide variety of uses, in this study the fine tuning of the weighting factors was based on the expert knowledge of the authors, with the intent of verify the overall accuracy of the model during the validation steps. Other target properties are found to be less sensitive to the weighting factors, and therefore are easier to match. The values adopted in the optimization process are also listed in Table 2.

The carbon type considered in the current study (CT1–11) are shown

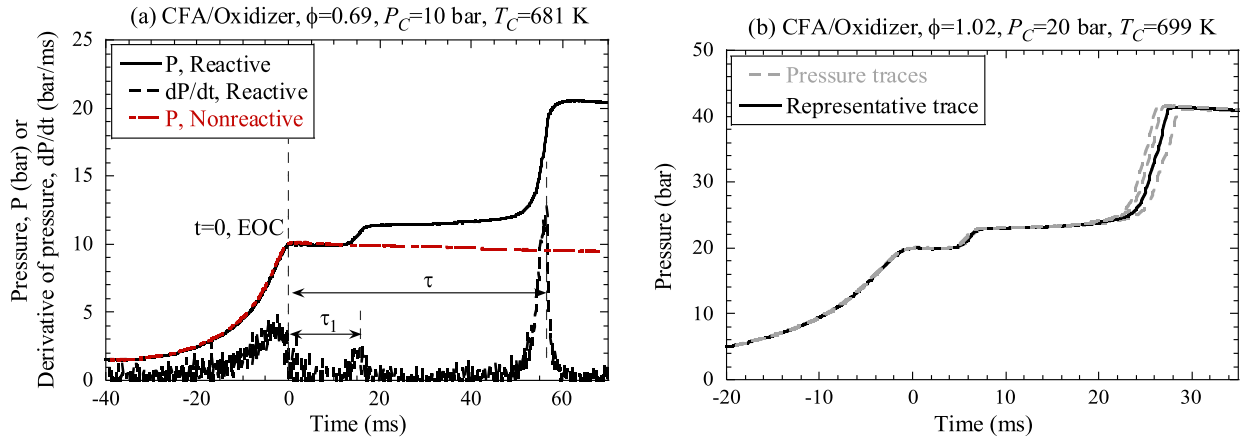


**Fig. 1.** RCM experiments of CFA diesel fuel: (a) definitions of first-stage and total ignition delay times ($\tau_1$ and $\tau$, respectively) at $P_C$ = 10 bar, $T_C$ = 681 K, and ϕ = 0.69 with dilution; (b) pressure traces at $P_C$ = 20 bar, $T_C$ = 699 K, and ϕ = 1.02 with dilution showing the experimental repeatability of the current study.

**Table 2**
Target property values [3,10] and weighting factors used for optimization of surrogate.

| | Target Value | Weighting Factors |
|---|---|---|
| H:C | 1.782 | 3.0 |
| DCN | 44.3[a] | 4.0 |
| Liquid density | 0.848 g/cm$^3$ | 3.0 |
| Advanced distillation curve | see Table 3 | 12.0 |
| Carbon type | see Table 3 | 4.0 |
| Yield sooting index | 122.2 | 0.1 |

[a]This value is the average of two derived cetane number (DCN) measurements reported in Fig. 6 of Mueller et al. [3].

**Table 3**
Target values [3,10] for advanced distillation curve and carbon type.

| Advanced Distillation Curve | Target Value [ °C] | Carbon Type | Target Value [mole fraction of carbon[a]] |
|---|---|---|---|
| 0 % | 224 | CT1 | 0.176 |
| 5 % | 232 | CT2 | 0.260 |
| 10 % | 237 | CT3 | 0.057 |
| 15 % | 241 | CT4 | 0.254 |
| 20 % | 247 | CT5 | 0.037 |
| 25 % | 250 | CT6 | 0.008 |
| 30 % | 254 | CT7 | 0.115 |
| 35 % | 259 | CT8 | 0.046 |
| 40 % | 263 | CT9 | 0.025 |
| 45 % | 267 | CT10 | 0.022 |
| 50 % | 271 | CT11 | 0 |
| 55 % | 274 | | |
| 60 % | 280 | | |
| 65 % | 284 | | |
| 70 % | 291 | | |
| 75 % | 297 | | |
| 80 % | 305 | | |
| 85 % | 316 | | |
| 90 % | 331 | | |

[a] Measurements by nuclear magnetic resonance spectroscopy, see discussion in Section 2.3.1 of Mueller et al. [10].

in Fig. 2 and follow those defined in [3,10]. It needs to be mentioned that the reason that the mole fraction of CT11 is found to be zero is because this carbon type was not detected in the target diesel fuel.CT11 is nevertheless included in the carbon types used in the current study, as one of the palette compounds, isocetane or 2,2,4,4,6,8,8-heptamethylnonane (HMN), contains a significant fraction of CT11, as mentioned in [10]. The advanced distillation curve has been simulated by a phase equilibrium/bubble-point model similar to that used by Huber et al. [25] and Kim et al. [27]. For vapor pressures, Antoine semi-empirical

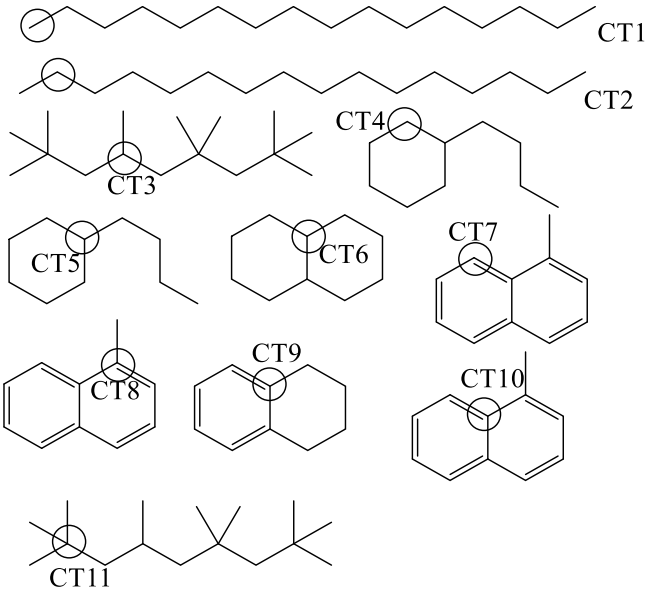


**Fig. 2.** Plot showing the definitions of carbon types (CT1–11) used in the current study. The definitions of CTs' have been adopted from Mueller et al. [3,10].

formulas for component vapor pressures [30] have been employed, with the Antoine equation coefficients for each surrogate palette component being taken from Yaws' Handbook [31]. The use of the empirical fits for vapor pressures has been validated by comparing the simulated distillation curves to multiple datasets measured by Bruno and co-workers [3,10,25,26,28,29]. Fig. 3 shows the results of the current method compared with the measured values of the CRC diesel surrogates of V0a, V0b, and V1 given by Mueller et al. [3]. A constant offset of 4.9 % is used to represent the fuel transit in the advanced distillation curve measurement. The need to offset the simulated data is consistent with the findings of Huber et al. [25]. Specifically, according to Eq. (2), the target function for the volatility data is defined as:

$$f_{ADC}(\vec{x}) = \frac{1}{N_{ADC}} \sum_{j=1}^{N_{ADC}} \left| \frac{T_m - T_s}{T_m} \right|, \quad (3)$$

where $N_{ADC}$ is the number of the measured points in the advanced distillation curve data, $T_m$ is the measured temperature for a given recovered volume, and $T_s$ is the estimated surrogate temperature at the matching recovered volume. Although the experimental distillation

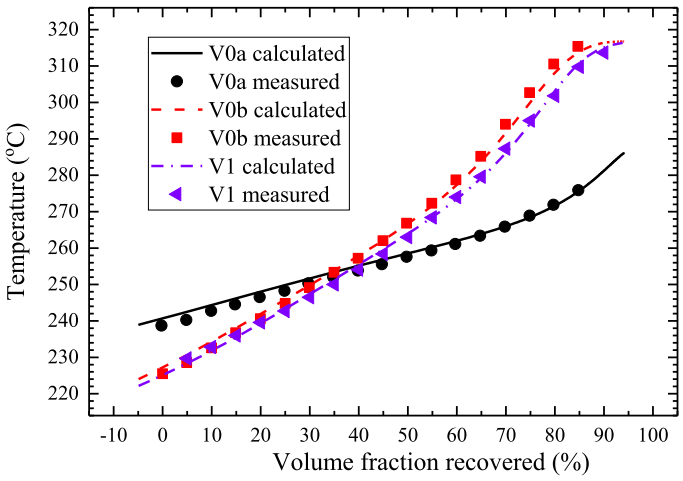


**Fig. 3.** Plot showing comparisons of the experimental and simulated distillation curves of CRC surrogates V0a, V0b, and V1. The experimental distillation curve data of CRC surrogates were taken from Mueller et al. [3].

curve of the surrogate mixture formulated in this study is not available, as it can be observed from Fig. 3 that the simulated distillation curves match well with the experimental ones, we can reasonably deduce that the simulated distillation curve for the current diesel surrogate is expected to have a good agreement with its experimental result.

*Surrogate palette*

Identification of the specific components to include in a surrogate formulation, referred to as the surrogate palette, is a critical and complex step in the surrogate formulation. Although it is expected that the molecules that make up the surrogate palette should be representative of those present in the target fuel, the components found in diesel fuels exhibit complex structural characteristics difficult to reproduce using a limited set of components, as shown in Farrell et al. [32]. For instance, the alkylbenzenes and mono-cycloparaffins observed in diesel fuels are primarily multi-alkyl substituted, which are difficult to obtain commercially and can be solid at room temperature, and hence it is challenging to study them in experimental facilities such as flow reactors, RCMs, and shock tubes. While it may be possible to develop reaction models to describe the chemical kinetics of such complex molecules by analogy to better-studied molecules or from the first-principle calculations, the fidelity of such kinetic models would be highly uncertain due to the lack of experimental validation data. Furthermore, recent works [5,33,34] have shown that surrogates, which are formulated to replicate compositional characteristics such as molecular class distribution, carbon type, and ignition ratings (e.g., octane number and DCN) of the target fuel, can be sufficient to emulate the ignition characteristics. Therefore, a surrogate palette selected in the current study, which comprises of molecules representing the different hydrocarbon classes and carbon types and with better-known ignition chemistry for developing reliable kinetic models, has been shown in Table 4 along with the key properties of the surrogate constituents. The abbreviations of palette compounds listed in Table 4 are used to denote the surrogate components starting from this section, to be consistent with the species names adopted in the current diesel surrogate model which will be introduced in Section 4.3. As the DCNs in Table 4 are measured following ASTM D6890 [35], their repeatability, or 95 % confidence interval, is stated as 0.01215 × (DCN+3.5).

The compounds TETRA, T124MBZ, A2CH3, PBZ, and C6H5C4H9 are chosen as the representatives of aromatics. TETRA is the simplest representative of the naphtho-aromatic hydrocarbons found in diesel and provides a source of carbon types 4, 7, and 9. A2CH3 has been used previously as a diesel reference fuel and is chosen here to represent the

**Table 4**
Properties of the components of the surrogate palette used in the current study.

| IUPAC Name (Kinetic Model Name) | CAS No. | H:C | DCN | Molecular Class | US Dollar |
|---|---|---|---|---|---|
| *n*-Dodecane (NC12H26) | 112–40–3 | 2.17 | 73.5[a] | *n*-Alkane | $130[d]/ 500 ml |
| *n*-Tetradecane (NC14H30) | 629–59–4 | 2.14 | 85.1[a] | *n*-Alkane | $190[d]/ 500 ml |
| *n*-Hexadecane (NC16H34) | 544–76–3 | 2.13 | 100[a] | *n*-Alkane | $198[d]/ 500 ml |
| *n*-Octadecane (NC18H38) | 593–45–3 | 2.11 | 106[b] | *n*-Alkane | $54[d]/ 100 g |
| *n*-Eicosane (NC20H42) | 112–95–8 | 2.10 | 110[b] | *n*-Alkane | $65[d]/ 100 g |
| *2,2,4,4,6,8,8*-Heptamethylnonane (HMN) | 4390–04–9 | 2.13 | 15[a] | isoAlkane | $350[d]/ 500 ml |
| *n*-Butylcyclohexane (NBCH) | 1678–93–9 | 2.00 | 47.6[a] | Cycloalkane | $407[d]/ 500 ml |
| *trans*-Decalin (DECALIN) | 91–17–8 | 1.80 | 31.8[a] | Cycloalkane | $95[e]/ 10 g |
| Tetralin (TETRA) | 119–64–2 | 1.20 | 8.9[a] | Naphtho-aromatic | $75[e]/ 500 ml |
| *1,2,4*-Trimethylbenzene (T124MBZ) | 95–63–6 | 1.33 | 8.9[a] | Aromatic | $35[d]/ 500 ml |
| *1*-Methylnaphthalene (A2CH3) | 90–12–0 | 0.91 | 0[a] | Aromatic | $82[f]/ 500 ml |
| *n*-Propylbenzene (PBZ) | 103–65–1 | 1.33 | 16[a,c] | Aromatic | $305[d]/ 500 ml |
| *n*-Butylbenzene (C6H5C4H9) | 104–51–8 | 1.40 | 12[a] | Aromatic | $300[e]/ 500 ml |

[a] DCNs reported in Yanowitz et al. [36].
[b] DCNs reported in Yanowitz et al. [37].
[c] Experimental cetane number using blend method.
[d] From Thermo Fisher Scientific.
[e] From Sigma Aldrich.
[f] From TCI America.

diaromatics found in diesel, thus providing a source of carbon types 7, 8, and 10. T124MBZ, PBZ, and C6H5C4H9 have been chosen as the representatives of alkylaromatics and also provide sources of carbon types 1, 2, 7, and 8. DECALIN and NBCH have been identified as the representatives of cycloalkanes which constitute about 35 % by weight in diesel [3], and act as sources of carbon types 1, 2, 4, 5 and 6. Similarly, NC12H26, NC14H30, NC16H34, NC18H38, and NC20H42 have been chosen as the representatives of the *n*-alkanes which make up about 15 % by weight in diesel fuels [3]. In addition, HMN has been chosen as the representative of the isoalkanes. The isoalkanes found in diesel are generally lightly branched (mono or dimethyl substitute alkanes) in contrast to the highly branched nature of HMN. Despite this difference, HMN has been selected for a variety of reasons: (a) HMN is a reference fuel for diesel cetane number measurement, (b) chemical kinetic models for dimethyl substituted alkanes like those in diesel are not currently available, (c) ignition propensity of large *2*-methylalkanes ($C_{10}$–$C_{20}$), which are more representative than HMN in terms of the types of branched alkanes found in commercial diesel fuels [3], are known to be very similar to their *n*-alkane counterparts, and (d) *2*-methylalkanes may require custom synthesis and are expensive to purchase. It is expected that the oxidation behavior of branched alkanes in the target fuel can be mimicked by a combination of HMN and different *n*-alkanes from the current surrogate palette. Furthermore, HMN provides a unique feature of exhibiting a low cetane rating along with a high H:C ratio. On the other hand, aromatics generally have low cetane ratings, and including higher amounts of aromatics would hinder matching the H:C. The benefits of choosing HMN in the palette will be shown in the following sections.

## Results and discussion

### *Surrogate formulation of CFA*

As described in Section 3, the surrogate formulation is generated via minimization of an objective function in Eq. (1). This has first been attempted via the gradient-free, local Nelder-Mead algorithm and random initialization of the surrogate composition. This initial approach shows that many local minima exist for the objective function as defined by the chosen surrogate palette, target properties, and target weights. To overcome this, both basin-hopping and evolutionary algorithm approaches have been tested. The basin-hopping technique has been found to consistently obtain the lowest objective function values and has been used in developing the final surrogate along with multiple random initializations using Latin hyper-cube sampling. Multiple local minima were also noted in the work of Huber et al. [26] in which they reported success via selection of multiple starting guesses. The basin-hopping method used here is a more reliable method than random-initialization for finding good objective function fitness. Due to the number of components in the present surrogate palette chosen to match all the desired target properties, global minimization by brute force is infeasible. As a result, the selected surrogate compositions cannot be considered to be global optima but are the best that are found by the present optimization methodology as codified in the objective function and weighting values as described in Section 3.1. All optimization algorithms used herein are those implemented within the scipy.optimize, a Python-based open--source framework [38].

Surrogates are generated using the current palette (Table 4) with and without the inclusion of HMN as one of the fuel components, and both surrogate compositions are shown in Table 5. Several major changes have been observed when varying the species and molar percentages from the optimized diesel surrogate to the one without HMN, such as the molar percentage of TETRA has decreased from 13.9 % to 6.7 %, the molar percentage of A2CH3 has increased from 17.7 % to 26.1 %, and the addition of C6H5C4H9 as another fuel component. Those changes in species and molar percentages in the surrogate without HMN are also targeted at matching the physical and chemical properties listed in Tables 2 and 3. By comparing the experimental distillation curve of CFA and the simulated distillation curves of the optimized surrogates with and without HMN, as shown in Fig. 4, we can conclude that the diesel surrogate with HMN provides a simulated volatility that better matches the curve of CFA. In addition, the optimized surrogate including HMN provides a better match to H:C, DCN, and density, as shown in Table 6, with the differences being less than 1 %.

Based on the information shown in Fig. 4, Tables 5 and 6, the optimized surrogate generated with HMN in the palette has been selected to be the final diesel surrogate from the current study. In Fig. 4, the distillation curves of the optimized surrogate and CFA consistently show a difference of about 15 K. This difference is partly due to the restriction imposed on the amounts of NC18H38 and NC20H42 in the surrogate formulation. As NC18H38 and NC20H42 are solids at room temperature and could potentially solidify under high pressures (an issue typically encountered in fuel injectors), an upper limit of 5 % (by weight) in the surrogate has been set to mitigate this problem. This constraint could also be contributing to the differences at the heavy end of the distillation curve. The other reason for the observed distillation curve differences could be due to the limitations of the current surrogate palette. From our simulations tests, it appears that addition of a component with a reasonable H:C (~1.6), low DCN (<20), and boiling point around 250 °C could result in a better matched distillation curve. It is to be noted that the properties of the diesel surrogates shown in Table 6 are estimated based on blending rules and are not experimentally determined. Comparisons with experimentally determined values for liquid density, cloud point, final melting point, and cetane number are provided in Section 4.2.

The comparison of carbon type distribution between the optimized surrogate and CFA are shown in Fig. 5. It is seen that the final surrogate closely reproduces the amounts of carbon types 1, 2, 4, and 7, which are the dominant carbon types (~80 % of carbon content) found in CFA.

**Table 5**
Compositions of the LLNL diesel surrogates with and without HMN.

| Surrogate with HMN | Molar percentage | Surrogate without HMN | Molar percentage |
|---|---|---|---|
| NC16H34 | 13.7 | NC16H34 | 11.0 |
| NC18H38 | 3.5 | NC18H38 | 2.8 |
| NC20H42 | 3.47 | NC20H42 | 2.6 |
| TETRA | 13.9 | TETRA | 6.7 |
| A2CH3 | 17.7 | A2CH3 | 26.1 |
| HMN | 20.5 | – | – |
| DECALIN | 20 | DECALIN | 17.8 |
| NBCH | 7.24 | NBCH | 7.24 |
| | | C6H5C4H9 | 1.7 |

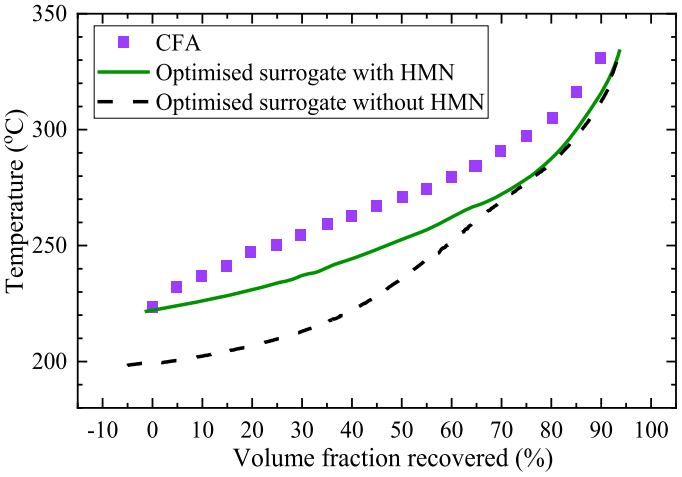


**Fig. 4.** Comparison of the distillation curves of CFA and the optimized surrogates with and without HMN in the palette.

**Table 6**
Comparison of the properties of CFA [3,10] and the estimated properties of the optimized surrogates (based on blending rules) with and without HMN.

| Property | CFA | Surrogate without HMN | Surrogate with HMN |
|---|---|---|---|
| DCN | 44.3 | 46.4 | 43.8 |
| H:C | 1.782 | 1.6 | 1.779 |
| Liquid density (g/cm$^3$) | 0.848 | 0.86 | 0.834 |

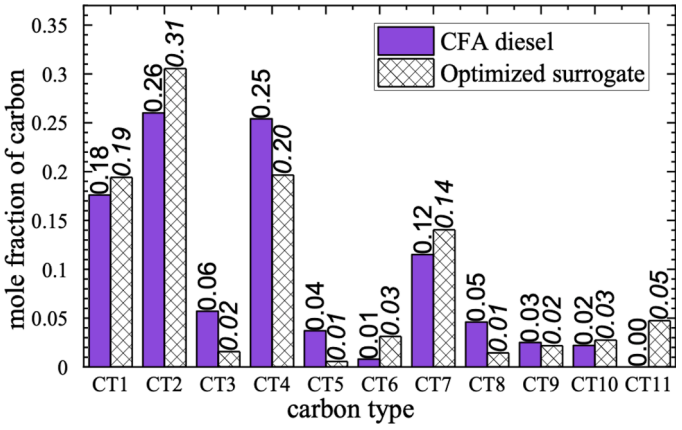


**Fig. 5.** Plots showing the carbon type distribution comparison for CFA [3,10] and the final optimized surrogate.

However, the final surrogate contains lower amounts of carbon types 3 and 5, which correspond to tertiary carbons found in straight-chain and alkylated cycloalkanes, respectively. Using quantitative structure–property relation regression, Won et al. [34] showed that the tertiary carbon type has an insignificant effect on the surrogate reactivity. It was found in [34] that the surrogate reactivity is mainly controlled by the $(CH_2)_n$ groups followed by the primary ($CH_3$) and benzyl groups. In the final surrogate, the carbon type 2 largely reflects the amounts of $(CH_2)_n$ groups, while the carbon type 1 reflects the amounts of the ($CH_3$) and benzyl groups. Hence, the observed differences in the carbon types are not expected to play an important role in affecting the ignition propensity of the final surrogate.

*Testing of physical and chemical properties of CFA diesel and optimized surrogate*

Several physical and chemical properties of the final diesel surrogate, denoted as LLNL diesel surrogate, were measured at the National Renewable Energy Laboratory to compare with those of the target diesel, as shown in Table 7. The properties of the CFA diesel fuel shown in Table 7 were taken from the CRC works [3,10]. The density of the surrogate is measured in accordance with the ASTM D4052 [39] test protocol, while the cloud point and final melting point are measured in compliance with the ASTM D5773 [40] protocol. As seen in Table 7, the density of the surrogate matches well with that of the target fuel, but the cloud point and final melting point of the surrogate show significant differences. However, according to the cloud point and final melting point comparisons with CFA and the CRC diesel surrogates shown in Fig. 6(a), the current LLNL diesel surrogate seems to perform better than the popular surrogates in the literature. This higher cloud point and final melting point of the current LLNL diesel surrogate can be attributed to the constraints put on the amount of NC18H38 and NC20H42 during the surrogate optimization. As mentioned previously, constraining the amounts of NC18H38 and NC20H42 also affects the distillation curve. It is seen from the comparison between the simulated distillation curve of LLNL diesel surrogate and the experimental distillation curve of CFA and CRC surrogates in Fig. 6(b) that the LLNL diesel surrogate evaporates at lower temperatures compared to most of the CRC surrogates. Even though the experimentally measured distillation curve of LLNL diesel surrogate is not available, it can be accurately predicted by the simulated distillation curve shown in Fig. 6(b), as has been mentioned earlier in the description and discussion of Fig. 3.

The ignition propensity of the LLNL diesel surrogate has also been measured based on the indicated cetane number (ICN) per the ASTM D8183 [41] protocol using an Advanced Fuel Ignition Delay Analyzer (AFIDA). As seen from Table 7, the ICN of the surrogate fuel (45.4) matches closely with the DCN of the target fuel (44.3) with an observed difference of ~1.1 cetane units which is within the experimental reproducibility of the DCN measured using the ASTM D6890 [35] protocol that is about ±2.85 cetane units for a fuel with DCN of 45. It is also to be noted that we are comparing the cetane ratings determined using two different ASTM protocols, but it is known that the ICN obtained from the ASTM D8183 [41] protocol is equivalent to the DCN measured using the ASTM D6890 [35] protocol, and the differences between the two protocols are not expected to be significant for DCN in the range of 35–55.

**Table 7**
Comparison of the measured properties of CFA and the LLNL diesel surrogate.

| Property | CFA [3] | LLNL diesel surrogate |
|---|---|---|
| Liquid density (g/cm$^3$) | 0.848 | 0.844 |
| Cloud point ( °C) | −19.2 | −5.1 |
| Final melting point ( °C) | −18.1 | −2.9 |
| Cetane number | 44.3 (DCN) | 45.4 (ICN) |

*Surrogate kinetic model*

A surrogate model describing the chemical kinetics of all the palette components listed in Table 4 has been assembled by merging the different new models developed at LLNL over the past three years and the $C_0$–$C_4$ base mechanism from AramcoMech 2.0 [42]. The combustion kinetics of A2CH3, T124MBZ, and TETRALIN were taken from recently published LLNL mechanisms [43,44]. The chemical kinetic models of DECALIN and NBCH were taken from the studies of Wang et al. [45] and Pitz et al. [46], respectively. In addition, the *n*-alkane mechanism of Kukkadapu et al. [47] describing the kinetics of $C_8$–$C_{20}$ *n*-alkanes and the HMN mechanism of Ritcher et al. [48] have been adopted. All the kinetic sub-models used to generate the diesel surrogate mechanism have been built using the state of art understanding of the oxidation pathways and have included the updated thermochemistry. Interested readers can find detailed information on the reaction pathways and the associated thermochemistry in [42–48]. This chemical kinetic mechanism consists of 6407 species and 20,180 reactions and has been included in Supplementary Material.

Furthermore, all the sub-models used to generate the current surrogate model have been validated against literature data, and some of the ignition delay time validations for pure and multicomponent mixtures of the surrogate components are shown in Fig. 7 and Fig. 8, respectively, where calculations are compared with experimental data from [7,43,45,49–57]. The current surrogate model generally does a very good job in capturing the ignition delay times of pure components with an average difference in ignition delay times of around 30 %, and with the largest discrepancies being around a factor of 2.

The performance of the model is less satisfactory for the binary fuel blends shown in Fig. 8. These discrepancies may be due to the inaccurate prediction of the consumption of smaller radicals such as OH and $HO_2$ radicals between the two fuels, as has also been mentioned in the study of Dames et al. [58] and Wang et al. [59]. The distribution of OH and $HO_2$ consumption and production by different fuel components in the LLNL diesel surrogate will also need to be demonstrated in future work to better understand the chemical kinetic interactions among fuels. The effect of cross-reactions among TETRA, HMN, and their fragments has also been studied in Wang et al. [59] using the current diesel surrogate model, and their results showed that cross-reactions of fuel fragments during combustion of high-/low-reactivity fuel blends are not necessary to be considered in the model, which is also consistent with the statements in Dames et al. [58]. Despite the discrepancies between experiment and simulation results for binary fuel blends, this model seems to do a much better job in predicting the reactivity of the complex multicomponent mixtures as shown in Fig. 8(c) for the CRC diesel surrogates of V0a, V0b and V1, with the ignition delay times predicted by the current mechanism are generally within ±30 % of the RCM measurements. A possible explanation for the better performance of this mechanism for the multicomponent mixtures in Fig. 8(c) in respect to the binary ones, is the higher concentrations of A2CH3 in the two component blends. Any discrepancies in predicting the reactivity of a single component in a binary mixture can affect simulations of the fuel blend severely. However, surrogate fuels which emulate physical and chemical characteristics of transportation fuels are generally multicomponent mixtures (e.g., V0a, V0b, V1, and the surrogate recommended in this work) and for these multicomponent mixtures, the sensitivity of the results to deficiencies in the kinetic model of a single component tend to affect less the predictions. Further validation of the mechanism against ignition delay times of the CRC surrogates can be found in [7]. This ability of the chemical kinetic model to accurately predict the reactivity of the multicomponent CRC surrogates containing up to eight components offers confidence in conclusions drawn on the fidelity of the current LLNL diesel surrogate composition in emulating autoignition of complex diesel fuels.

It is worth noting that discrepancies of ignition delay times between measurement and the simulated results from the current diesel surrogate

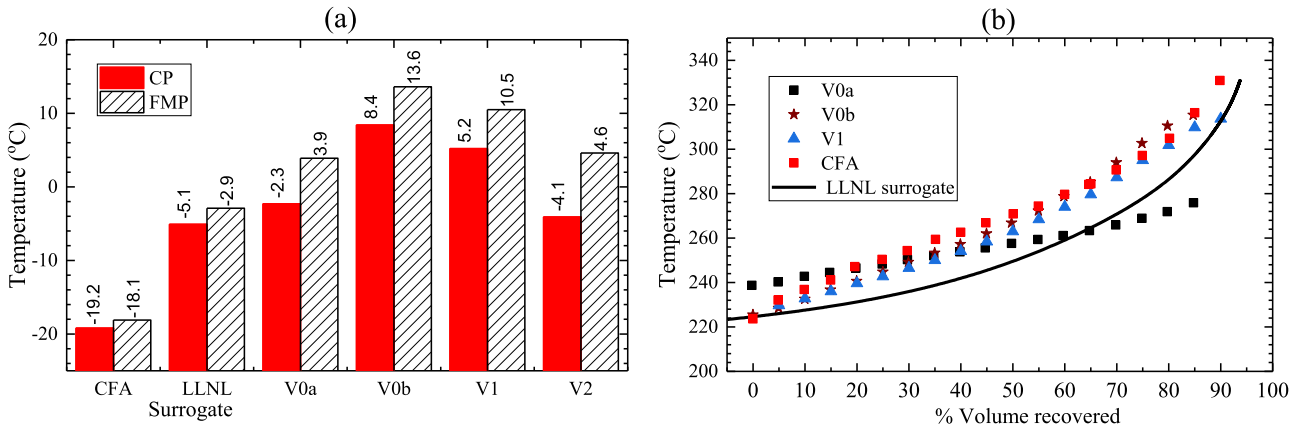


**Fig. 6.** Comparisons of (a) cloud point (CP) and final melting point (FMP) and (b) distillation curve for the target CFA diesel fuel and the surrogates from the current study and CRC. The properties of CFA and CRC surrogates (V0a, V0b, V1) were taken from Mueller et al. [3,10].

model can be partially attributed to uncertainties of the simulated results. Assigning uncertainties of the simulated results would require as a minimum an assessment of overall rate constants, branching ratios, and thermodynamic properties. While uncertainty quantification techniques can provide a more rigorous assessment of the potential outcomes from a kinetic model, it is beyond the scope of this study. As previous work on a gasoline surrogate fuel by Fridlyand et al. [60] suggested that the overall autoignition uncertainty was primarily attributable to the fuel-specific low-temperature chemistry reactions, it is reasonable to believe that a study focusing on diesel surrogate fuels would arrive at the same conclusion. Due to the complex non-linear nature of uncertainty quantification and being it outside the scope of this work, we refrain from assigning a more quantitative uncertainty to the simulations shown throughout this study.

*Comparison of experimental data and surrogate modeling results*

Fig. 9 shows the comparison of the experimental ignition delay times of CFA obtained using an RCM and the simulated results using the current surrogate model, at varying temperatures, pressures, fuel concentrations, and oxygen concentrations. Here, all the RCM ignition delay time simulations are obtained using the volume history generated from the corresponding nonreactive experiment (by replacing $O_2$ with $N_2$) capturing the heat transfer effects during the compression stroke and the post-compression period. Further details about the nonreactive experiments and the generation of volume histories can be found in [20,21]. The volume histories, reactive pressure histories, and ignition delay time datasets for all the test conditions have been made available in Supplementary Material. In addition, the representative comparisons between the experimental and simulated time-resolved pressure histories are shown in Fig. S1 in Supplementary Material.

As can be observed from Fig. 9, the current surrogate model correctly predicts the experimental trends, with the total ignition delay times of CFA decreasing monotonically with increasing pressure, fuel concentration, and oxygen concentration. In addition, Fig. 9 shows that the total ignition delay times are correctly reproduced by the surrogate model, with about two thirds of the simulated ignition delay times inside the error bars. The limited deviations observed consist, generally, in shorter ignition delay times at low temperatures (<700 K) and in the negative temperature coefficient (NTC) regime, and longer ignition delays for intermediate temperatures (>800 K). Regarding first-stage ignition delay time comparisons, the surrogate model captures the characteristic dependence of first-stage ignition delay times on variations in fuel concentration, equivalence ratio and pressure accurately, and the differences between experimental and simulated results in first-stage ignition delay time predictions are similar to the those of total ignition delay times. In addition, it has been noticed in Fig. 9(b) that the experimental first-stage ignition delay times do not vary with the effect of fuel concentration at a fixed $O_2$ concentration. One possible reason may be due to the minor fuel molar percentage change (0.36 % to 0.51 %) in the fuel concentration effect while the molar percentages of $O_2$ and $N_2$ remain almost the same, as reported in Table 1. In this case, the heat release rate before first-stage ignition also remains largely the same. As the first-stage ignition delay time is mainly controlled by the unimolecular decomposition of ketohydroperoxides, which is a reaction pathway with relatively high activation energy and its reaction rate strongly depends on temperature, the heat release rate can be a major factor controlling the rate of this reaction, thus determining the first-stage ignition delay times. Therefore, the fuel concentration effect will not noticeably affect the first-stage ignition delay times, as can be observed in Fig. 9(b).

To further assess the predictive capabilities of the current surrogate model in emulating the ignition propensity of different diesel blends at various temperature regimes, the total ignition delay times of a Chinese Stage VI diesel fuel from the RCM study of Yu et al. [14] and the shock tube study of a Europe DF2 diesel fuel from Haylett et al. [61] have been compared against the current modeling predictions, with the results shown in Fig. 10(a) and Fig. 10(b), respectively. It has to be pointed out that the comparisons of experimental ignition delay times, cetane ratings, and compositions of those literature diesel fuels [14,61] to those of a #2 ULSD certification fuel have been included in our previous work [7]. As the chemical properties of Chinese Stage VI diesel studied by Yu et al. [14], including DCN, CN, and the weight percentages of hydrocarbon classes, are different compared to those of ULSD#2 diesel, for validations of the current surrogate mechanism we used the five-component surrogate formulation suggested by Yu et al. [14], and the simulations in Fig. 10(a) have been conducted using the diesel surrogate mechanism developed in the current study. Since the autoignition behavior of the diesel blend used by Haylett et al. [61] is close to that of ULSD#2 at high temperature, we use the LLNL surrogate for the simulations. It can be seen in Fig. 10(a) that the simulation results using the current model have good agreement with the experimental results of [14], especially in the NTC regime. As seen from Fig. 10(b), the predicted total ignition delay times closely match with the experimental values reported by Haylett et al. [61] at temperatures above 1050 K. For temperatures below 1050 K, the model seems to be slightly less reactive than the experiments (~30 % over-prediction in ignition delay time), which is consistent with the comparisons against the total ignition delay time data from the current RCM experiments. Some of the discrepancies observed between the experiments and simulations in Fig. 10(b) could also be linked to the large uncertainties in the data, due to the complicated fuel loading process in the aerosol shock tube of [61].

Finally, it should be noted that the current study is one of the first which demonstrates the efficacy of detailed kinetic models in

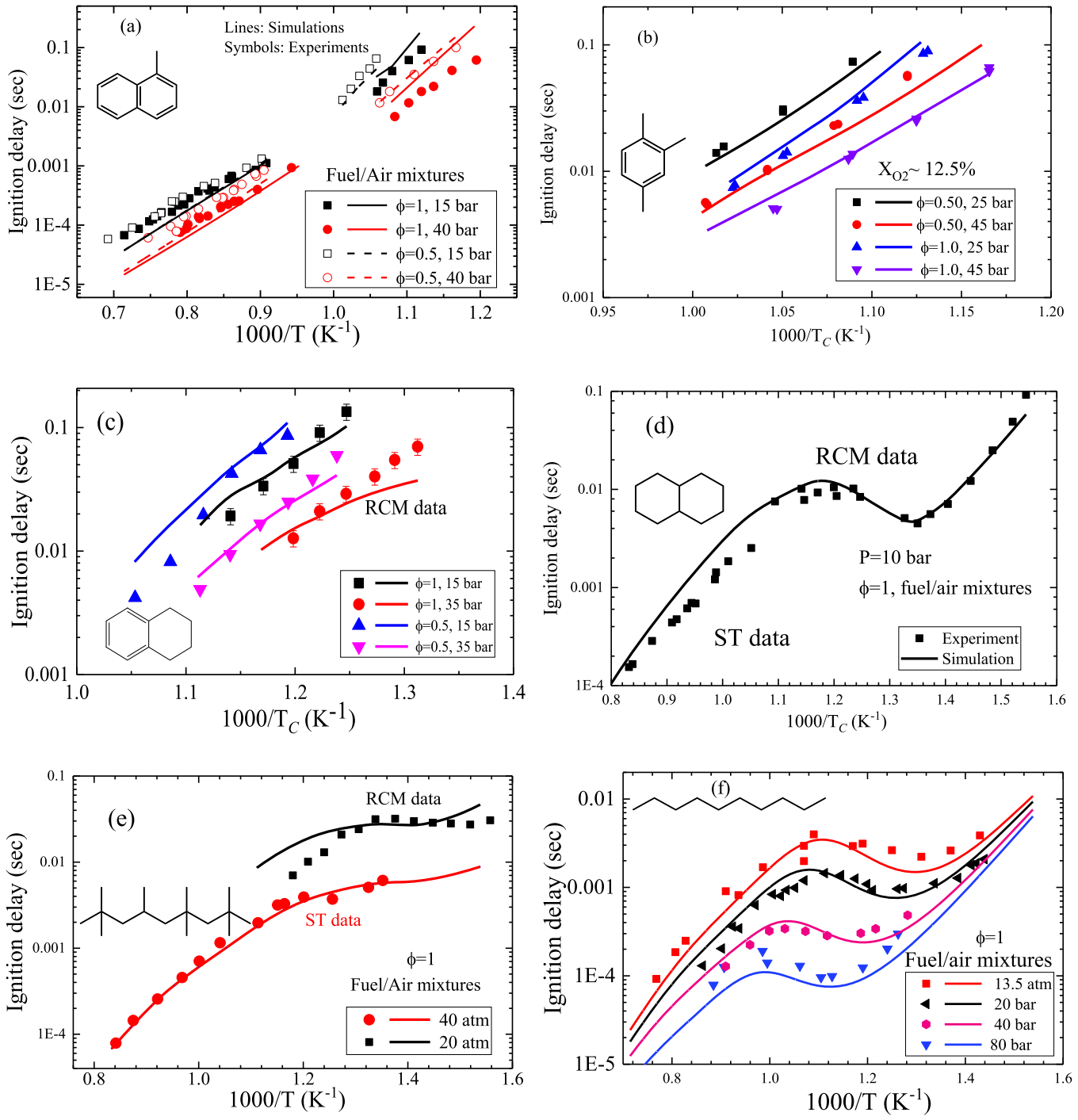


**Fig. 7.** Plots comparing the experimental RCM and shock tube (ST) data and simulated total ignition delay times of (a) A2CH3, (b) T124TMB, (c) TETRA, (d) DECALIN, (e) HMN, and (f) *n*-decane. The experimental data (symbols) are taken from [43,45,49–57]. Zero-dimensional reactor simulations (lines) with and without volume histories are used to model RCM and ST data, respectively.

successfully simulating the ignition characteristics of diesel fuels. The current surrogate model does a very good job in qualitatively emulating the ignition response of the CFA diesel fuel to changes in temperature, pressure, oxygen concentration, and fuel concentration. As such, the level of agreement in the experimental and simulated ignition delay times observed herein is encouraging and the current surrogate model can provide insights into ignition chemistry of diesel under engine-relevant conditions. Finally, the mechanism demonstrated to be able to simulate ignition characteristics of different diesel fuel blends.

*Chemical kinetic analyses*

Brute force sensitivity analyses have been performed under constant volume adiabatic (CONV) simulations based on the current diesel surrogate model, at $\phi = 0.5$ in air and $\phi = 1$ with dilution, initial pressure of 10 bar, and initial temperature of 750 K, to identify the controlling chemistry for autoignition. The sensitivity analysis results are shown in Fig. 11. In order to facilitate the sensitivity analyses, the total ignition delay time in the present CONV simulations is defined as the time at which the local temperature is 400 K above the initial temperature and

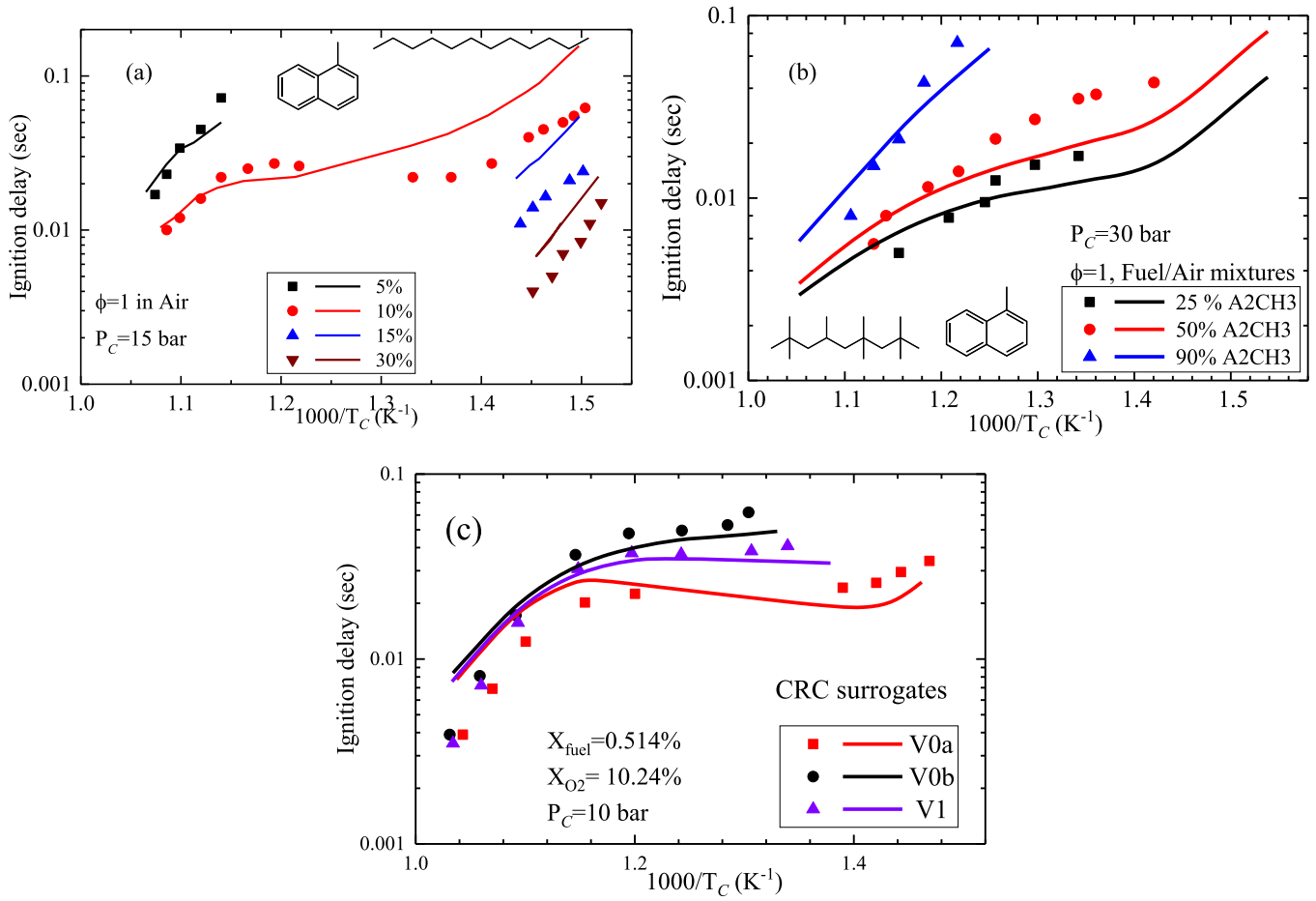


**Fig. 8.** Plots comparing the RCM experimental (symbols) and simulated (lines) total ignition delay times of (a) NC12H26/A2CH3 blends, (b) HMN/A2CH3 blends, and (c) CRC surrogates. The experimental data shown in (a) and (b) are taken from [57], while those of (c) are taken from [7]. Percent values shown in legends are on molar basis. Zero-dimensional reactor simulations with volume histories are used to model RCM data.

the first-stage ignition as the time when a 10 K temperature increase is recorded. The relative total ignition delay sensitivity coefficient ($S_{rel}$) is defined as $S_{rel} = \ln(\tau_+/\tau)/\ln(k_+/k)$, where k and $\tau$ are the unperturbed reaction rate constant and the corresponding original total ignition delay time, respectively, and $k_+$ is the rate constant increased by a factor of two while $\tau_+$ is the resulting total ignition delay time. The sensitivity analyses for first-stage ignition delay time are also carried out in the same manner. Therefore, a reaction with a positive sensitivity coefficient inhibits reactivity while one with a negative sensitivity coefficient promotes reactivity.

Another sensitivity analysis was completed to investigate the effect of compositional changes in the surrogate mixture at $\phi = 0.5$ in air, initial pressure of 10 bar, and initial temperature of 750 K. The molar composition of the final optimized surrogate shown in Fig. 5 is defined as the nominal surrogate mixture. For each perturbed mixture simulated, the mole fraction of a single fuel component was increased by 0.1 (absolute). For each perturbation, the remaining seven components have a proportionally reduced mole fraction. For these eight perturbed mixtures, the total and first-stage ignition delay times were extracted from the simulations and the sensitivity of the mixture to each component is defined as $S = \frac{\tau(perturbed) - \tau(nominal)}{\tau(nominal)}$ for total ignition delay times and first-stage ignition delay times. The results are shown in Fig. 12.

For the total ignition delay time sensitivity analysis of the LLNL diesel surrogate, Fig. 11(a) shows the top-ranked most sensitive reactions. The decomposition of $H_2O_2$ (R38) is a major reaction promoting reactivity, and other most dominant reactions are among smaller intermediate species. The H-abstraction reactions by OH radicals involving surrogate components are also controlling the autoignition chemistry, with reactions of A2CH3, DECALIN, and TETRA forming TETRARB (R32, R29, and R23) promoting the reactivity, and with H-abstraction reactions of HMN forming HMN-R5 (R9) and TETRA forming TETRARS (R11) inhibiting the reactivity. The inhibiting effect of R9 is due to the inability of tertiary QOOH radicals to further produce ketohydroperoxides (KHPs) through the subsequent propagation reactions. The inhibiting effect of R11 is due to the propensity of tetralyl peroxy radicals formed from TETRARS to participate in the concerted elimination reactions forming C10H10 and $HO_2$, reducing the reactivity of the radical pool, as discussed in Wang et al. [7]. Other fuel-component-related reactions promoting the reactivity include the formation of KHPs (R22, R27) and isomerization reactions of alkylperoxy ($RO_2$) radicals forming QOOH radicals from DECALIN (R19, R20), and the reactions inhibiting the reactivity include the concerted elimination reactions of $RO_2$ radicals from DECALIN and TETRA (R10, R12, R16).

For the sensitivity results based on perturbations to the surrogate composition in Fig. 12, it can be observed that five components show enhancing effects on the reactivity of total ignition, except for HMN, A2CH3, and TETRA which effectively reduce reactivity. The acceleration of total ignition delay time is most pronounced by increasing the molar percentages of *n*-alkanes. This promoting effect on reactivity is not shown in Fig. 11(a), which may be due to the limited mole fractions of *n*-alkanes (less than 20 %) in the optimized surrogate mixture proposed in this work.

Unlike the sensitivity analysis results on total ignition delay time, where the most dominant reactions involve smaller intermediate

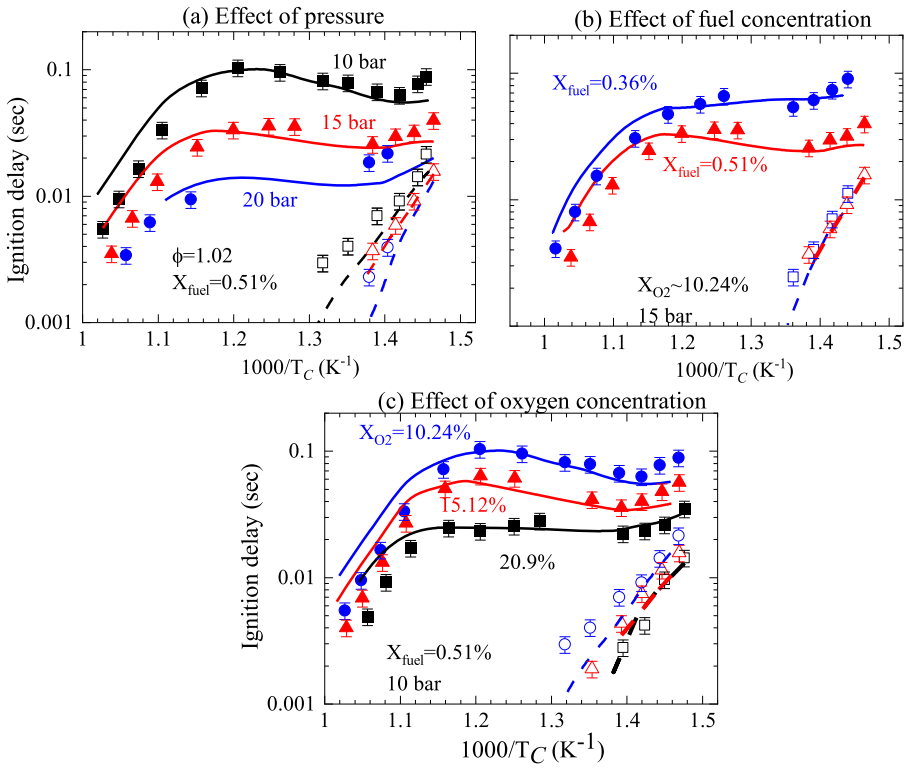


**Fig. 9.** Comparison of the experimental ignition delay times (symbols) of CFA diesel fuel and the simulated results (lines) using the current surrogate model at (a) varying pressures, (b) fuel concentrations, and (c) oxygen concentrations. Error bars represent $a \pm 15$ % in measured ignition delay time. Filled symbols/solid lines are for total ignition delay times, while open symbols/dashed lines are for first-stage ignition delay times.

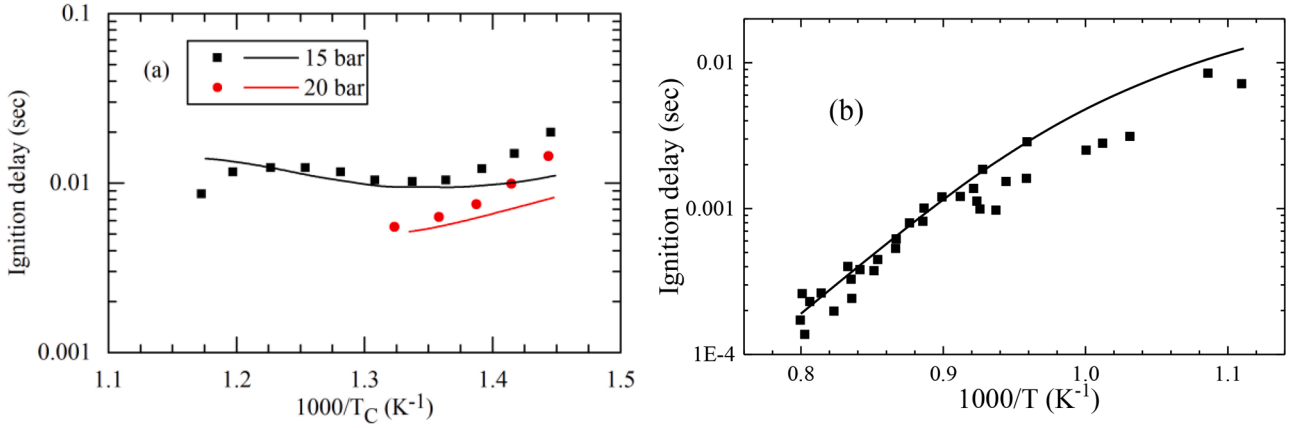


**Fig. 10.** Comparison of the experimental total ignition delay times (symbols) of diesel fuels and the simulated results (lines) using the current surrogate model – (a) RCM experiments from Yu et al. [14] and simulations using five-component surrogate suggested by Yu et al. [14] at $P_C = 15$ and 20 bar, $\phi = 1.25$ with an oxidizer of 10.5 % $O_2$ in $N_2$, and (b) Shock tube experiments from Haylett et al. [61] and simulations using LLNL surrogate at $P = 6$ atm, $\phi = 0.5$ with an oxidizer of 21 % $O_2$ in Ar. Simulations include $dP/dt = 3$ %/ms in the shock tube experiments.

species, the top-ranked reactions controlling the reactivity of first-stage ignition at the same test condition are among fuel-related species, which can be seen in Fig. 11(b). The H-abstraction reactions of NC16H34 and TETRA by OH are the most dominant reactions promoting and inhibiting the reactivity of first-stage ignition, respectively. This is consistent with the pronounced accelerating and retarding effect on first-stage ignition by adding additional 10 % molar percentage of NC16H34 and TETRA, respectively, as shown in Fig. 12. In addition, it can be observed that the H-abstraction reactions of fuel components, such as HMN, A2CH3, and DECALIN, by OH radicals also have positive first-stage sensitivity coefficients. Consistently with Wang et al. [7] findings, in diesel like blends *n*-alkanes are the first components to be consumed (mainly by abstraction by OH radicals) participating in the low temperature oxidation. Their degenerate branching path boosts the OH radical production accelerating the oxidation of the fuel. Increased amounts of DECALIN, A2CH3, TETRA, and HMN offer alternative targets for the OH abstractions, distracting them from attacking the more reactive compounds, resulting in a retarding effect on first-stage ignition.

Table 8 shows the consumption and production of OH and $HO_2$ radicals from the major reaction pathways of each fuel component and their radicals. This analysis is conducted via CONV simulations for the same initial condition as the percent sensitivity analysis in Fig. 12 at 1 % conversion of HMN, which is prior to the onset of first-stage ignition. About 99 % of OH radicals are consumed by the LLNL diesel surrogate

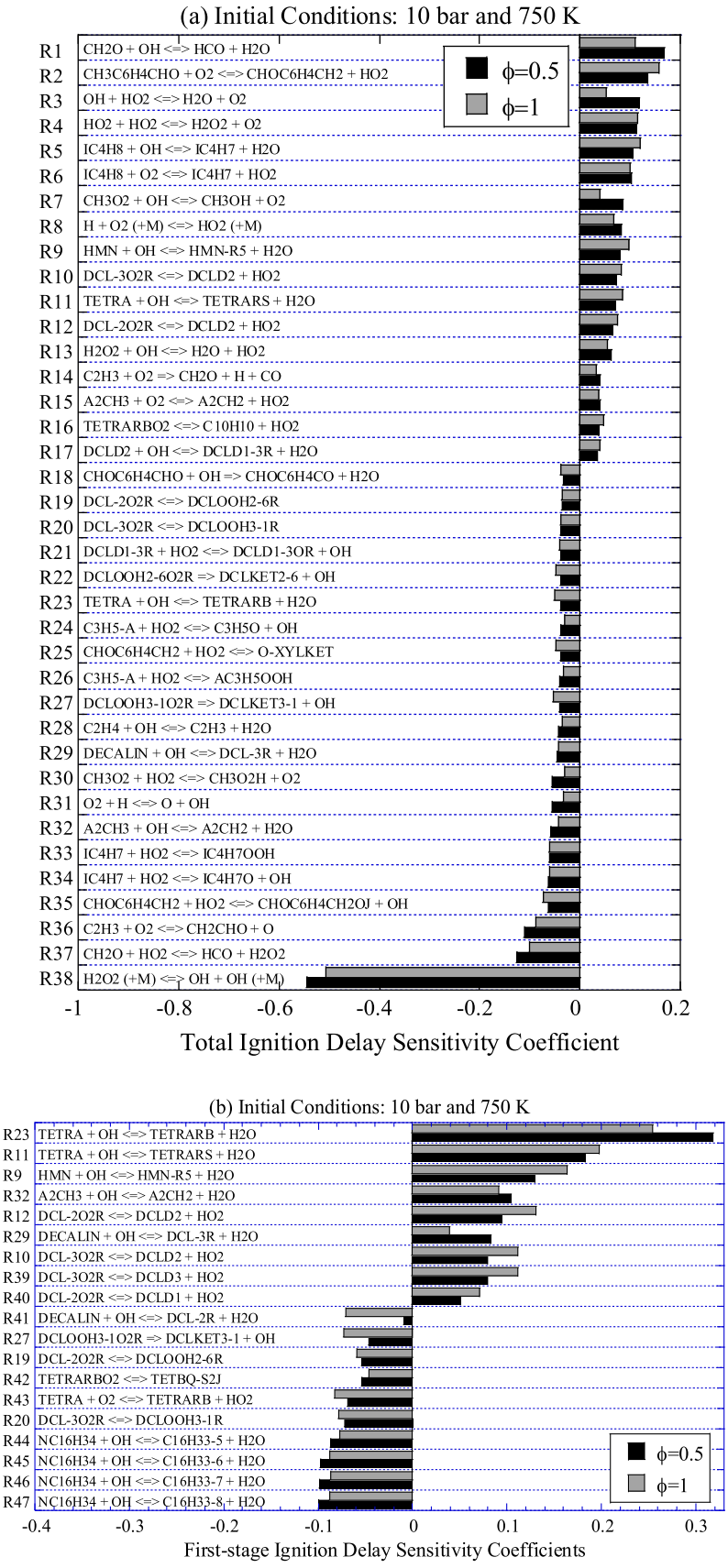


**Fig. 11.** Brute force sensitivity coefficients for (a) total and (b) first-stage ignition delay times of LLNL diesel surrogate at $\phi = 0.5$ in air and $\phi = 1$ with dilution, initial pressure of 10 bar, and initial temperature of 750 K.

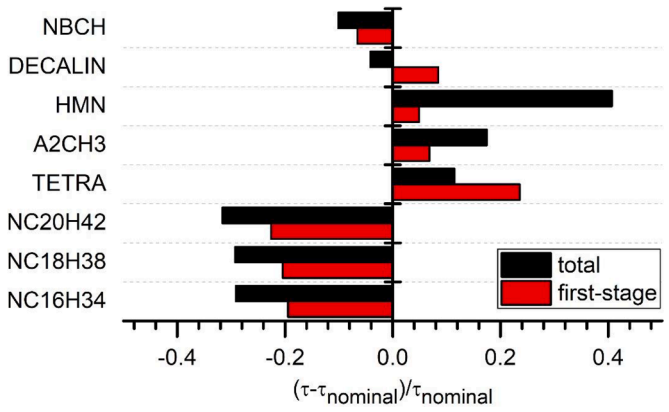


**Fig. 12.** Total and first-stage ignition delay time sensitivities to perturbations in the nominal surrogate composition with initial conditions of 750 K and 10 bar at $\phi = 0.5$ in air for CONV simulations. See main text for details.

components via H-abstraction reactions, and 78 % OH radicals are produced by fuel components and their radicals via the major reactions such as low temperature chain branching reactions, including the formation and decomposition of KHPs and hydroperoxyl cyclic ethers, cyclic ethers formation, etc. It can be concluded from the OH production/consumption ratio in Table 8 that *n*-alkanes and NBCH produce more OH radicals than their consumption. This trend is consistent with the negative sensitivity values shown in Fig. 12.

Abstractions by $HO_2$, followed by decomposition of $H_2O_2$, is another major source of OH radicals, as can also be seen in Fig. 11(a). About 34 % of the total consumption of $HO_2$ can be attributed to abstractions on fuel components, producing $H_2O_2$. Reactions involving fuel components and their radicals account for about 62 % of the total $HO_2$ production, including the major reactions such as the H-abstraction by $O_2$, the concerted elimination by $RO_2$ and QOOH radical decomposition. $HO_2$ radicals can also be consumed by reacting with smaller species, always leading to the formation of $H_2O_2$, as can be seen in Fig. 11(a). It can be observed in Table 8 that alkanes produce more $HO_2$ radicals than they consume, while aromatics (TETRA, A2CH3) consume more $HO_2$ radicals than they produce. We can further see in Table 8 that the ratio of OH production to OH consumption by TETRA and A2CH3 is less than 40 % indicating they are strong OH radical scavengers. However, n-alkanes and NBCH are relative sources of OH production with ratios that exceed 100 % in Table 8. Components such as HMN and DECALIN are also scavengers of OH radicals with ratios of ~66 %. HMN also has a retarding effect on both first-stage and total ignition according to Fig. 12, which may be due to more consumption of OH radicals than its production, and the production of $HO_2$ radicals being the same as its consumption. We can also conclude from Table 8 that the $HO_2$ production/consumption ratio of DECALIN is the highest among fuel components.

Further inspection of Table 8 helps to explain the change in sign of the sensitivity associated with DECALIN in Fig. 12. At an initial temperature of 750 K, until first-stage ignition occurs DECALIN serves as an OH radical scavenger owing to a low ratio of OH production to consumption. However, after first-stage of ignition occurs and the temperature of the system increases, DECALIN begins producing more $HO_2$ than it consumes. At intermediate temperatures, such as those post first-stage ignition, $HO_2$ will typically participate in H-atom abstraction reactions forming $H_2O_2$. It is well known that at such temperatures $H_2O_2$ then quickly decomposes to two OH radicals effectively increasing the reactivity of the system. Hence, DECALIN can simultaneously delay the first-stage ignition time and reduce the overall ignition delay time as shown in Fig. 12.

## Some observations

As diesel fuels contain a large number of with large and structurally complex fuel molecules, the development of chemical kinetics able to simulate their behavior can be of great value. In Section 4.5, Figs. 11 and 12, it is clearly shown how the structural features of diesel fuel molecules can affect the overall reactivity by controlling the evolution of the radical pool before the onset of autoignition (particularly of OH, and $HO_2$, the main players in the low to intermediate temperature region, 600–950 K). For this reason, having a good understanding of the chemical kinetics of those structures can better help controlling the overall rate of real diesel fuel autoignition.

The present study represents a step forward in the detailed chemical kinetic modeling of practical transportation fuels, which began with realistic high temperature mechanisms for straight-chain, saturated fuels such as *n*-heptane and branched fuels such as isooctane. The development of such models progressed steadily including unsaturated fuels, alcohol fuels, including the butanol isomers, and more recently, to alcohol and many other oxygenates from biomass and large biodiesel fuels. In parallel, the range and complexity of practical applications for the kinetic mechanisms has greatly expanded, from high temperature shock tube ignition to laminar flames, low temperature ignition, and engine knocking simulations. The present study extends the degree of realism of surrogate fuel models available for autoignition simulations of diesel combustion by incorporating a deeper understanding of the chemical kinetic emerging from the compositional complexity of diesel fuels. The results of the present study will also benefit future kinetic studies of similar complexities found in jet fuels.

Past modeling effort established that it was possible to combine models for many *n*-alkane hydrocarbon fuels [62,63], and many related isoalkane fuels [64], into single detailed kinetic mechanisms. In both cases, reliable simulations were possible for larger fuel components with the smaller ones embedded within the base mechanism, but without inclusion of fuels with more complex structure. Our more recent development [65–67] extended the same capabilities to include virtually any number of simultaneous fuel types (i.e., alkane, olefin, alcohol, oxygenate, aromatic, etc.) into a single chemical kinetic mechanism, with the simulations showing the communication of each fuel via their different reaction histories of various radicals and stable intermediate chemical species. That is, each fuel component produces its own distribution and amounts of radicals and stable intermediate species, and those radicals/species can subsequently react with any other stable or

**Table 8**
Consumption and production of OH and $HO_2$ from the major reactions of each fuel component at 1 % conversion of HMN under the same initial condition as Fig. 12.

| Species names | OH consumption | OH production | OH production/OH consumption | $HO_2$ consumption | $HO_2$ production | $HO_2$ production/$HO_2$ consumption |
|---|---|---|---|---|---|---|
| NC16H34 | 24.6 % | 25.7 % | 104.5 % | 2 % | 14.5 % | 604.2 % |
| NC18H38 | 7.1 % | 7.4 % | 104.2 % | 0.7 % | 4.1 % | 585.7 % |
| NC20H42 | 7.9 % | 8.4 % | 106.3 % | 0.8 % | 4.4 % | 550 % |
| TETRA | 10.1 % | 2.7 % | 26.7 % | 17 % | 14 % | 82.4 % |
| A2CH3 | 2.5 % | 1 % | 40 % | 8.2 % | 0% | 0 % % |
| HMN | 19.8% | 13 % | 65.7 % | 1.4 % | 1.4 % | 100 % |
| DECALIN | 21.7 % | 14.5 % | 66.8 % | 3.1 % | 21.6 % | 696.8 % |
| NBCH | 5 % | 5.4% | 108 % | 0.8 % | 2.1 % | 262.5 % |
| Total | 99 % | 78.1 % | 79.1 % | 34 % | 62.1 % | 182.6 % |

intermediate species to simulate at the test conditions resistant to engine knock. According to the principles demonstrated in this work, it is then possible to provide a single detailed chemical kinetic mechanism to describe the reactivity of many different real fuels.

## Conclusions

This study presents an optimized diesel surrogate mixture that improves the ability to match the chemical and physical properties in addition to the autoignition behavior of a target diesel fuel (CFA) with an associated detailed chemical kinetic model. The present study extends the degree of realism in fuels available for autoignition simulations of diesel combustion, provided by considerable extensions in better chemical kinetic understandings of diesel fuel compositional complexity. A surrogate mixture which closely emulates the chemical and physical properties of CFA has been formulated based on an optimization approach, and a detailed diesel surrogate model describing the ignition of the surrogate constituents was developed by matching physical and chemical characteristics of target diesel fuels in the current study, with the sub-model of each surrogate fuel component being well validated. The ignition delay time validations for pure fuel components and multicomponent blends of the surrogate components have been conducted by comparing with the literature experimental data, and the ignition delay times of the optimized surrogate computed using the current LLNL diesel surrogate model are further validated by comparing against the experimental data of CFA and the literature experimental data of other diesel fuels. The computed ignition delay times show that the surrogate formulation from the current study can qualitatively capture the ignition response of CFA to changes in pressure, oxygen concentration, and fuel concentration quite well. Furthermore, the experimental ignition delay times are generally well predicted by the surrogate model with differences less than 30 %, a metric that, in the context of this kind of modeling, is considered to be good agreement. Chemical kinetic analyses of the current LLNL diesel surrogate model, including sensitivity analyses and the consumption and production of OH and $HO_2$ radicals by various fuel components, have also been conducted to identify the key reactions controlling the autoignition chemistry and the distribution of smaller radicals by reacting with various fuel components.

The experimental ignition delay times of diesel associated with this work, the detailed kinetic model for diesel surrogate mixtures, as well as the chemical kinetic analyses of the current model can improve the understanding of diesel autoignition and combustion under a wide-range of conditions. Possible directions for modification to improve the detailed kinetic model and surrogate fuel mixture were also presented. The development of the detailed kinetic model in this work is, to our knowledge, one of the first that compiles well-validated sub-mechanisms of individual surrogate components representing hydrocarbon classes of complex diesel fuel into a single detailed reaction mechanism. The current study includes the addition of more realistic diesel surrogate components such as more complex naphthenic and aromatic components found in diesel fuels. The diesel surrogate model built in the current study is significantly better at simulating the behavior of the target CFA diesel fuel which is representative of commercial diesel fuel and commonly used in engine combustion research studies. In future work, more tests on this newly developed diesel surrogate, in both experiments and simulations, can be conducted to validate its ability to capture more physical and chemical properties of its target diesel. The methodology of surrogate formulation in the current work can also be further utilized and improved for future surrogates of different transportation fuels.

## Declaration of Competing Interest

The authors declare that they have no known competing financial interests or personal relationships that could have appeared to influence the work reported in this paper.

## Data availability

We have shared files in the Attach File step.

## Acknowledgments

The work at LLNL is supported by the U.S. Department of Energy, Office of Energy Efficiency and Renewable Energy, Vehicle Technologies Office (program manager, Mike Weismiller) and performed under the auspices of the U.S. Department of Energy by LLNL under Contract DE-AC52-07NA27344. The work at UConn was supported by the NSF under Grant No. CBET-1402231 and the LLNL via Standard Research Subcontract No. B621898. We also would like to thank CRC for providing the CFA diesel fuel.

## Supplementary materials

Supplementary material associated with this article can be found, in the online version, at doi:10.1016/j.jaecs.2023.100216.

## References

[1] Pitz WJ, Mueller CJ. Recent progress in the development of diesel surrogate fuels. Prog Energy Combust Sci 2011;37:330–50.
[2] Kundu P, Xu C, Som S, Temme J, Kweon CM, Lapointe S, Kukkadapu G, Pitz WJ. Implementation of multi-component diesel fuel surrogates and chemical kinetic mechanisms for engine combustion simulations. Transp Eng 2021;3:100042.
[3] Mueller CJ, Cannella WJ, Bays JT, Bruno TJ, DeFabio K, Dettman HD, Gieleciak RM, Huber ML, Kweon CB, McConnell SS, Pitz WJ, Ratcliff MA. Diesel surrogate fuels for engine testing and chemical-kinetic modeling: compositions and properties. Energy Fuels 2016;30:1445–61.
[4] Mehl M, Chen JY, Pitz WJ, Sarathy SM, Westbrook CK. An approach for formulating surrogates for gasoline with application toward a reduced surrogate mechanism for CFD engine modeling. Energy Fuels 2011;25:5215–23.
[5] Ahmed A, Goteng G, Shankar VSB, Al-Qurashi K, Roberts WL, Sarathy SM. A computational methodology for formulating gasoline surrogate fuels with accurate physical and chemical kinetic properties. Fuel 2015;143:290–300.
[6] Dooley S, Won SH, Heyne J, Farouk TI, Ju Y, Dryer FL, Kumar K, Hui X, Sung CJ, Wang H, Oehlschlaeger MA, Iyer V, Iyer S, Litzinger TA, Santoro RJ, Malewicki T, Brezinsky K. The experimental evaluation of a methodology for surrogate fuel formulation to emulate gas phase combustion kinetic phenomena. Combust Flame 2012;159:1444–66.
[7] Wang M, Kukkadapu G, Zhang K, Wagnon SW, Mehl M, Pitz WJ, Westbrook CK, Sung CJ. Autoignition of CRC diesel surrogates at low temperature combustion conditions: rapid compression machine experiments and modeling. Combust Flame 2020;219:178–97.
[8] Anand K, Ra Y, Reitz RD, Bunting B. Surrogate model development for fuels for advanced combustion engines. Energy Fuels 2011;25:1474–84.
[9] Chang Y, Jia M, Li Y, Liu Y, Xie M, Wang H, Reitz RD. Development of a skeletal mechanism for diesel surrogate fuel by using a decoupling methodology. Combust Flame 2015;162:3785–802.
[10] Mueller CJ, Cannella WJ, Bruno TJ, Bunting B, Dettman HD, Franz JA, Huber ML, Natarajan M, Pitz WJ, Ratcliff MA, Wright K. Methodology for formulating diesel surrogate fuels with accurate compositional, ignition-quality, and volatility characteristics. Energy Fuels 2012;26:3284–303.
[11] Jameel AGA, Naser N, Emwas AH, Sarathy SM. Surrogate formulation for diesel and jet fuels using the minimalist functional group (MFG) approach. Proc Combust Inst 2019;37:4663–71.
[12] Bai Y, Wang Y, Wang X, Wang P. Development of a skeletal mechanism for tri-component diesel surrogate fuel: n-hexadecane/iso-cetane/1-methylnaphthalene. Fuel 2020;259:116217.
[13] Qian Y, Yu L, Li Z, Zhang Y, Xu L, Zhou Q, Han D, Lu X. A new methodology for diesel surrogate fuel formulation: bridging fuel fundamental properties and real engine combustion characteristics. Energy 2018;148:424–47.
[14] Yu L, Wang S, Wang W, Qiu Y, Qian Y, Mao Y, Lu X. Exploration of chemical composition effects on the autoignition of two commercial diesels: rapid compression machine experiments and model simulation. Combust Flame 2019;204:204–19.
[15] Yu L, Mao Y, Li A, Wang S, Qiu Y, Qian Y, Han D, Zhu L, Lu X. Experimental and modeling validation of a large diesel surrogate: autoignition in heated rapid compression machine and oxidation in flow reactor. Combust Flame 2019;202:195–207.
[16] Wang S, Mao Y, Raza M, Yu L, Lu X. Autoignition of diesel /oxygen / nitrogen mixture under elevated temperature in a heated shock tube. Fuel 2019;254:115635.
[17] Zhu J, Zhou D, Yu L, Qian Y, Lu X. Construction of a skeletal multi-component diesel surrogate model by integrating chemical lumping and genetic algorithm. Fuel 2022;313:122711.

[18] Khodayari H, Ommi F, Saboohi Z. A review on the applications of the chemical reactor network approach on the prediction of pollutant emissions. Aircr. Eng. Aerosp. Technol. 2020;92/4:551–70.
[19] Lee D, Hochgreb S. Rapid compression machines: heat transfer and suppression of corner vortex. Combust Flame 1998;114:531–45.
[20] Das AK, Sung CJ, Zhang Y, Mittal G. Ignition delay study of moist hydrogen/oxidizer mixtures using a rapid compression machine. Int J Hydrog Energy 2012;37:6901–11.
[21] Kukkadapu G, Sung CJ. Autoignition study of ULSD# 2 and FD9A diesel blends. Combust Flame 2016;166:45–54.
[22] Desgroux P, Gasnot L, Sochet LR. Instantaneous temperature measurement in a rapid-compression machine using laser Rayleigh scattering. Appl Phys B Laser Opt 1995;61:69–72.
[23] Sung CJ, Curran HJ. Using rapid compression machines for chemical kinetics studies. Prog Energy Combust Sci 2014;44:1–18.
[24] Weber BW, Sung CJ, Renfro MW. On the uncertainty of temperature estimation in a rapid compression Machine. Combust Flame 2015;162:2518–28.
[25] Huber ML, Smith BL, Ott LS, Bruno TJ. Surrogate mixture model for the thermophysical properties of synthetic aviation fuel S-8: explicit application of the advanced distillation curve. Energy Fuels 2008;22:1104–14.
[26] Huber ML, Lemmon EW, Bruno TJ. Surrogate mixture models for the thermophysical properties of aviation fuel Jet-A. Energy Fuels 2010;24:3565–71.
[27] Kim D, Martz J, Violi A. A surrogate for emulating the physical and chemical properties of conventional jet fuel. Combust Flame 2014;161:1489–98.
[28] Reiter AM, Schubert N, Pfennig A, Wallek T. Surrogate generation and evaluation for biodiesel and its mixtures with fossil diesel. Energy Fuels 2017;31:6173–81.
[29] Bruno TJ, Smith BL. Evaluation of the physicochemical authenticity of aviation kerosene surrogate mixtures. Part 1: analysis of volatility with the advanced distillation curve. Energy Fuels 2010;24:4266–76.
[30] Antoine C. Tensions des vapeurs; nouvelle relation entre les tensions et les températures. C.R 1888;107:681–4. 778-780, 836-837.
[31] Yaws CL, Narasimhan PK, Gabbula C. Yaws' handbook of antoine coefficients for vapor pressure (2nd Electronic Edition). Knovel; 2009. Online version available at, http://app.knovel.com/hotlink/toc/id:kpYHACVPEH/yaws-handbook-antoine/yaws-handbook-antoine.
[32] Farrell JT, Cernansky NP, Dryer FL, Friend DG, Hergart CA, Law CK, McDavid RM, Mueller CJ, Patel AK, Pitsch H. Development of an experimental database and kinetic models for surrogate diesel fuels. SAE Technical Paper; 2007. 2007-01-0201.
[33] Sarathy SM, Kukkadapu G, et al. Compositional effects on the ignition of FACE gasolines. Combust Flame 2016;169:171–93.
[34] Won SH, Haas FM, Dooley S, Edwards T, Dryer FL. Reconstruction of chemical structure of real fuel by surrogate formulation based upon combustion property targets. Combust Flame 2017;183:39–49.
[35] Standard test method for determination of ignition delay and derived cetane number (DCN) of diesel fuel oils by combustion in a constant volume chamber. PA, USA: ASTM Standard D6890-13b; ASTM International: West Conshohocken; 2013. https://doi.org/10.1520/D6890.
[36] J. Yanowitz, M.A. Ratcliff, R.L. McCormick, J.D. Taylor, M.J. Murphy, Compendium of experimental cetane numbers, Technical Report NREL/TP-5400-67585, 2017.
[37] J. Yanowitz, M.A. Ratcliff, R.L. McCormick, J.D. Taylor, M.J. Murphy, Compendium of experimental cetane numbers, Technical Report NREL/TP-5400-61693, 2014.
[38] E. Jones, T. Oliphant, P. Peterson, others, SciPy: open source scientific tools for Python, 2001. http://www.scipy.org/.
[39] Standard test method for density, relative density, and API gravity of liquids by digital density meter, ASTM standard D4052-11. West Conshohocken, PA, USA: ASTM International; 2011. https://doi.org/10.1520/D4052.
[40] Standard test method for cloud point of petroleum products (constant cooling rate method), ASTM standard D5773-15. West Conshohocken, PA, USA: ASTM International; 2015. https://doi.org/10.1520/D5773.
[41] Standard test method for determination of indicated cetane number (ICN) of diesel fuel oils using a constant volume combustion chamber—reference fuels calibration method. ASTM Standard D8183-18; ASTM International: West Conshohocken, PA; 2018. https://doi.org/10.1520/D8183-18.
[42] Li Y, Zhou CW, Somers KP, Zhang K, Curran HJ. The oxidation of 2-butene: a high pressure ignition delay, kinetic modeling study and reactivity comparison with isobutene and 1-butene. Proc Combust Inst 2017;36:403–11.
[43] Kukkadapu G, Kang D, Wagnon SW, Zhang K, Mehl M, Goldsborough S, Pitz WJ, Palacios MM, Wang H. Kinetic modeling study of surrogate components for gasoline, jet and diesel fuels: C7-C11 methylated aromatics. Proc Combust Inst 2019;37:521–9.
[44] Issayev G, Djebbi K, Kukkadapu G, Mehl M, Wagnon SW, Pitz WJ, A Farooq. Experimental and kinetic modeling study of tetralin: a naphtheno-aromatic fuel for gasoline, jet and diesel surrogates. Proc Combust Inst 2021;38:641–9.
[45] Wang M, Zhang K, Kukkadapu G, Wagnon SW, Mehl M, Pitz WJ, Sung CJ. Autoignition of trans-decalin, a diesel surrogate compound: rapid compression machine experiments and chemical kinetic modeling. Combust Flame 2018;194:152–63.
[46] Pitz WJ, Liang J, Kukkadapu G, Zhang K, Conroy C, Bugler J, Curran HJ. A detailed chemical kinetic modeling and experimental investigation of the low- and high-temperature chemistry of n-butylcyclohexane. Int J Chem Kinet 2020;53:465–75.
[47] Kukkadapu G, Wagnon SW, Rodriguez A, Veloo PS, Mehl M, Westbrook CK, Mcnenly MJ, Sarathy SM, Herbinet O, Battin-Leclerc F, Sung CJ, Dooley S, Won SH, Dryer FL, Pitz WJ. An updated comprehensive chemical kinetic model of $C_8$-$C_{20}$ *n*-alkanes. 10th U.S. Natl Combust Meet 2017. paper 2RK-0500.
[48] Richter S, Kukkadapu G, Westbrook CK, Braun-Unkhoff M, Naumann C, Köhler M, Riedel U. A combined experimental and modeling study of combustion properties of an isoparaffinic alcohol-to-jet fuel. Combust Flame 2022;240:111994.
[49] Kukkadapu G, Sung CJ. Autoignition study of 1-methylnaphthalene in a rapid compression machine. Energy Fuels 2017;31:854–66.
[50] Kukkadapu G, Weber BW, Sung CJ. Autoignition study of tetralin in a rapid compression machine at elevated pressures and low-to- intermediate temperatures. Fuel 2015;159:436–45.
[51] Zhu Y, Davidson DF, Hanson RK. Pyrolysis and oxidation of decalin at elevated pressures: a shock-tube study. Combust Flame 2014;161:371–83.
[52] Oehlschlaeger MA, Steinberg J, Westbrook CK, Pitz WJ. The autoignition of iso-cetane at high to moderate temperatures and elevated pressures: shock tube experiments and kinetic modeling. Combust Flame 2009;156:2165–72.
[53] Yu L, Qiu Y, Mao Y, Wang S, Ryan C, Tao W, Qian Y, Lu X. A study on the low-to-intermediate temperature ignition delays of long chain branched paraffin: iso-cetane. Proc Combust Inst 2019;37:631–8.
[54] Pfahl U, Fieweger K, Adomeit G. Self-ignition of diesel-relevant hydrocarbon-air mixtures under engine conditions. In: Proceedings of the 26th international symposium on combustion; 1996. p. 781–9.
[55] Tekawade A, Xie T, Oehlschlaeger MA. Comparative study of the ignition of 1-decene, trans-5-decene and n-decane: constant-volume spray and shock-tube experiments. Energy Fuels 2017;31:6493–500.
[56] Zhukov VP, Sechenov VA, Starikovskii AY. Autoignition of n-decane at high pressure. Combust Flame 2008;153:130–6.
[57] Kukkadapu G, Sung CJ. Autoignition of binary blends of *n*-dodecane/*1*-methylnaphthalene and *iso*-cetane/*1*-methylnaphthalene. Combust Flame 2018;189:367–77.
[58] Dames EE, Rosen AS, Weber BW, Gao. C.J. Sung CW, Green WH. A detailed combined experimental and theoretical study on dimethyl ether/propane blended oxidation. Combust Flame 2016;168:310–30.
[59] Wang M, Kukkadapu G, Pitz WJ, Sung CJ. Autoignition study of *iso*-cetane/tetralin blends at low temperature. Combust Flame 2021;228:415–29.
[60] Fridlyand A, Johnson MS, Goldsborough SS, West RH, McNenly MJ, Mehl M, Pitz WJ. The role of correlations in uncertainty quantification of transportation relevant fuel models. Combust Flame 2017;180:239–49.
[61] Haylett DR, Lappas PP, Davidson DF, Hanson RK. Application of an aerosol shock tube to the measurement of diesel ignition delay times. Proc Combust Inst 2009;32:477–84.
[62] Westbrook CK, Pitz WJ, Herbinet O, Curran HJ, Silke EJ. A comprehensive detailed chemical kinetic reaction mechanism for combustion of *n*-alkane hydrocarbons from *n*-octane to *n*-hexadecane. Combust Flame 2009;156:181–99.
[63] Sarathy SM, Westbrook CK, Mehl M, Pitz WJ, Togbe C, Dagaut P, Wang H, Oehlschlaeger MA, Niemann U, Seshadri K, Veloo PS. Comprehensive chemical kinetic modeling of the oxidation of *2*-methylalkanes from $C_7$ to $C_{20}$. Combust Flame 2011;158:2338–57.
[64] Curran HJ, Gaffuri P, Pitz WJ, Westbrook CK. A Comprehensive modeling study of *iso*-octane oxidation. Combust Flame 2002;129:253–80.
[65] Herbinet O, Pitz WJ, Westbrook CK. Detailed chemical kinetic oxidation mechanism for a biodiesel surrogate. Combust Flame 2008;154:507–28.
[66] Mehl M, Pitz WJ, Westbrook CK, Curran HJ. Kinetic modeling of gasoline surrogate components and mixtures under engine conditions. Proc Combust Inst 2011;33:193–200.
[67] Cheng S, Saggese C, Kang D, Goldsborough SS, Wagnon SW, Kukkadapu G, Zhang K, Mehl M, Pitz WJ. Autoignition and preliminary heat release of gasoline surrogates and their blends with ethanol at engine-relevant conditions: experiments and comprehensive kinetic modeling. Combust Flame 2021;228:57–77.